

## **Correction of the IRD influence for paleo-current flow speed reconstructions in hemipelagic sediments**

**N. Stevenard<sup>1\*</sup>, A. Govin<sup>1</sup>, C. Kissel<sup>1</sup> & A. Van Toer<sup>1</sup>**

<sup>1</sup>Laboratoire des Sciences du Climat et de l'Environnement, LSCE/IPSL, CEA-CNRS-UVSQ, Université Paris-Saclay, Gif-sur-Yvette, France.

### **Contents of this file**

Text S1.  
Figures S1 to S5

### **Introduction**

This supplementary material explains in more details the results of XRF calibration for the North Atlantic cores. These calibrations follow the method proposed by (Weltje et al., 2015).

#### **Text S1.**

**Figures S1.** and **S2.** show correlations between elemental concentrations from the measured XRF (discrete samples) and predicted XRF (e.g. predicted by the calibration). Predicted rubidium (Rb) concentrations are significantly correlated to the “true” concentrations with a  $R^2$  of 0.9 and 0.91 for cores MD03-2679 and MD03-2673, respectively. Predicted zirconium (Zr) concentrations are significantly correlated to the “true” concentrations with a  $R^2$  of 0.69 and 0.89 for cores MD03-2679 and MD03-2673, respectively.

**Figure S3.** shows the distributions (%) in log-scale of each calibrated element over the studied period for the two North Atlantic cores.

**Figure S4.** shows profiles of  $\ln(\text{Zr}/\text{Rb})$  (calibrated),  $\text{Rb}_{\text{carb free}}$  and  $\text{Zr}_{\text{carb free}}$  for the two North Atlantic cores. In order to observe elemental variability of the detrital fraction, the biogenic carbonate ( $\text{CaCO}_3$ ) influence was removed from the  $\text{Rb}_{\text{carb free}}$  and  $\text{Zr}_{\text{carb free}}$  concentrations following the equation given by Poutiers and Gonthier (1978) and used by Kissel et al. (2013) ( $\text{concentration}\% / 100 - \text{CaCO}_3\%$ ). The  $\text{CaCO}_3$  concentrations were obtained with the assumption that Ca concentrations obtained by XRF measurements are representative of biogenic carbonate content.

**Figure S5.** Shows all grain-size distributions (a, c, e) and sand fraction profiles (b, d, f) of the three studied cores. The sortable silt interval is marked by light yellow areas in a, c, e. The percentile 80 (i.e. grain-size value below which 80% of the data is, also given in Table 2) of the average grain-size distribution is marked by red dotted lines in a, c, e.

#### References

- Kissel, C., Van Toer, A., Laj, C., Cortijo, E., & Michel, E. (2013). Variations in the strength of the North Atlantic bottom water during Holocene. *Earth and Planetary Science Letters*, 369–370, 248–259. <https://doi.org/10.1016/j.epsl.2013.03.042>
- Poutiers, J., Gonthier, E. (1978). Sur la susceptibilité magnétique des sédiments, indicateurs de la dispersion du matériel volcanoclastique à partir de l'Islande et des Faeroes. *Bull. Inst. Géol. Bassin Aquitaine*, 23, 214–226.
- Weltje, G. J., Bloemsma, M. R., Tjallingii, R., Heslop, D., Röhl, U., & Croudace, I. W. (2015). Prediction of Geochemical Composition from XRF Core Scanner Data: A New Multivariate Approach Including Automatic Selection of Calibration Samples and Quantification of Uncertainties. In I. W. Croudace & R. G. Rothwell (Eds.), *Micro-XRF Studies of Sediment Cores* (Vol. 17, pp. 507–534). Dordrecht: Springer Netherlands. [https://doi.org/10.1007/978-94-017-9849-5\\_21](https://doi.org/10.1007/978-94-017-9849-5_21)

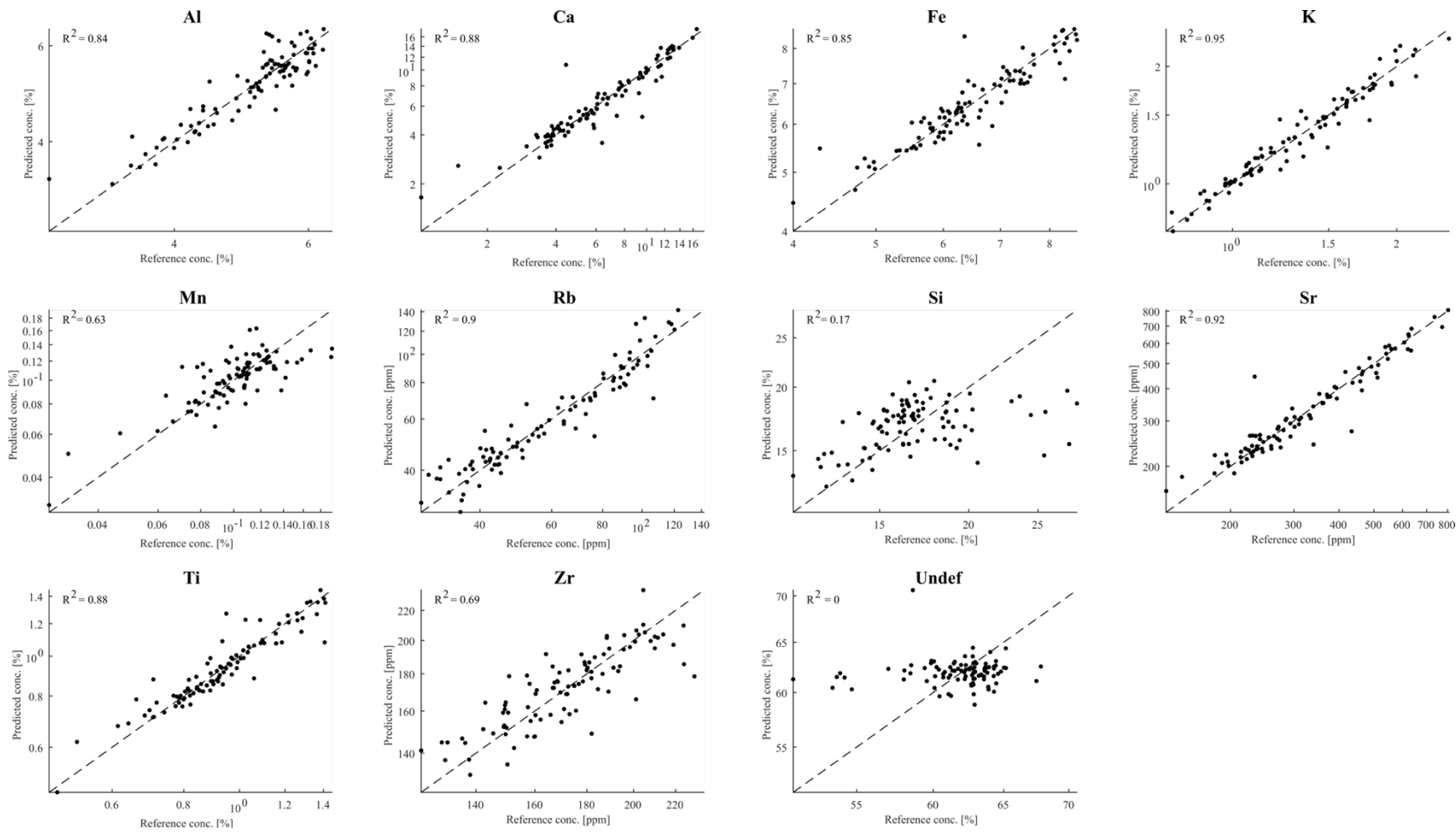


**Figure S1.** Correlations for core MD03-2679 between elemental concentrations directly measured on discrete samples (using ED-XRF) and predicted concentrations obtained on core-scanner data after running the Multivariate log-ratio calibration (Weltje et al. 2015).

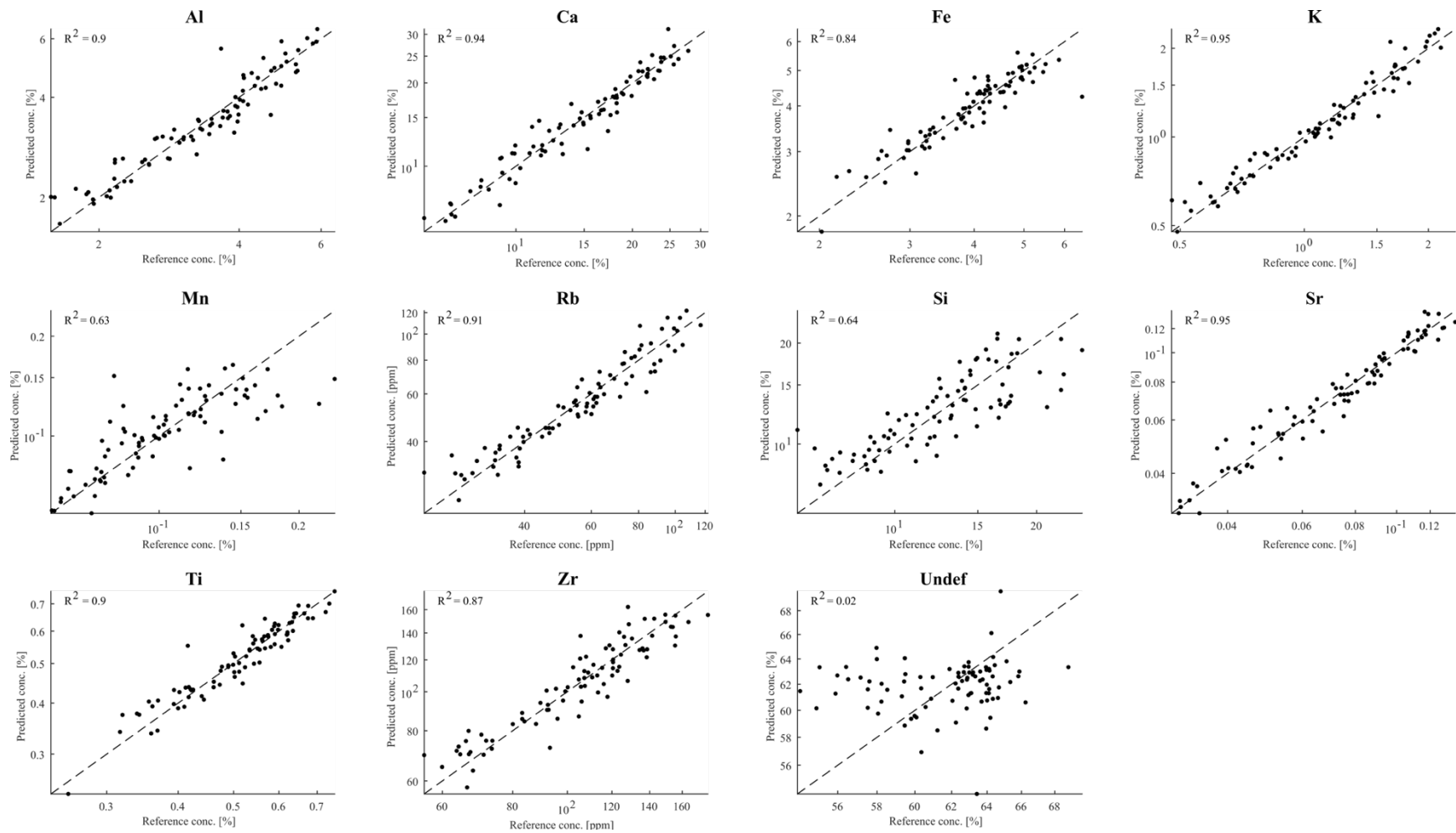
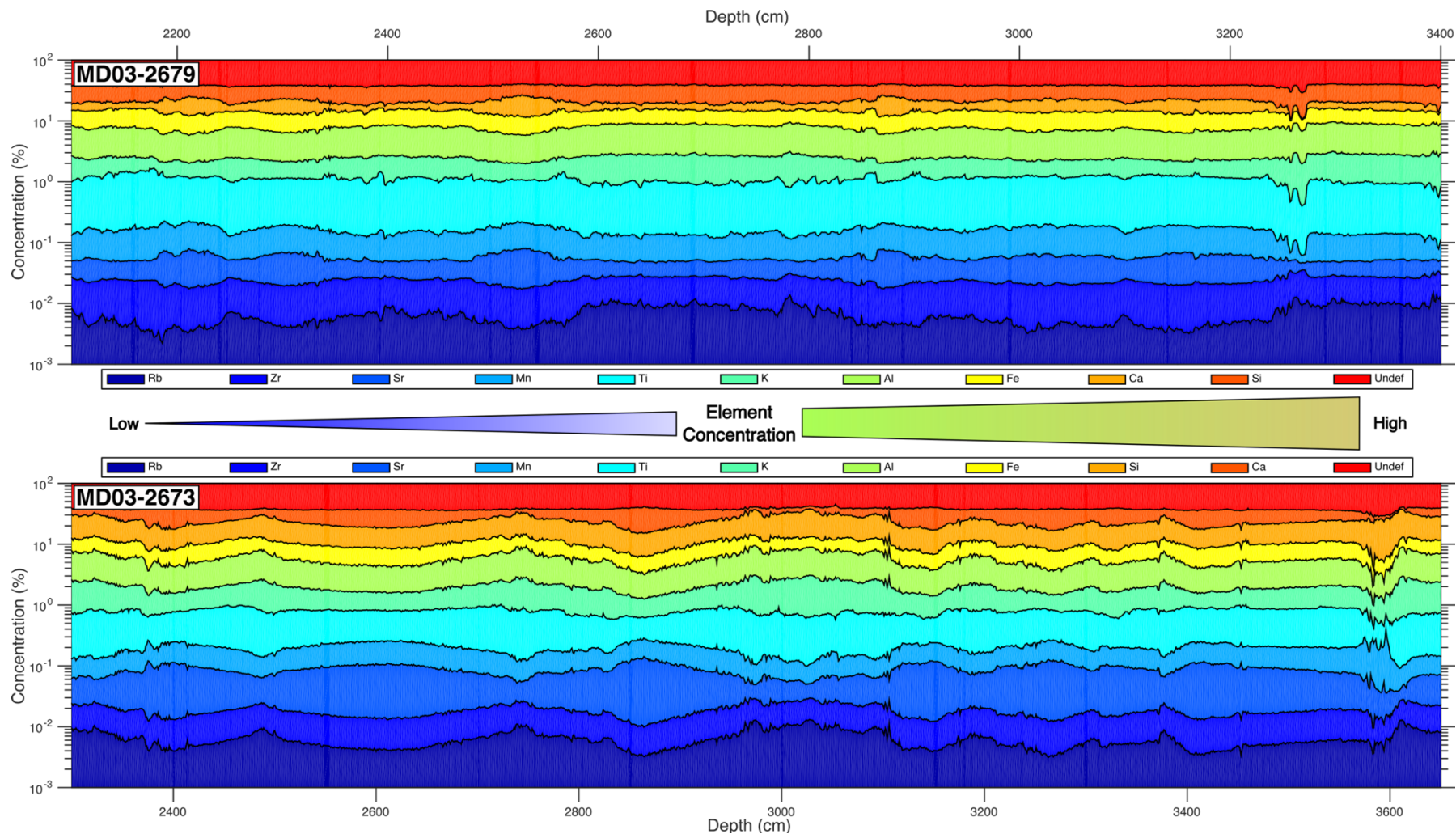
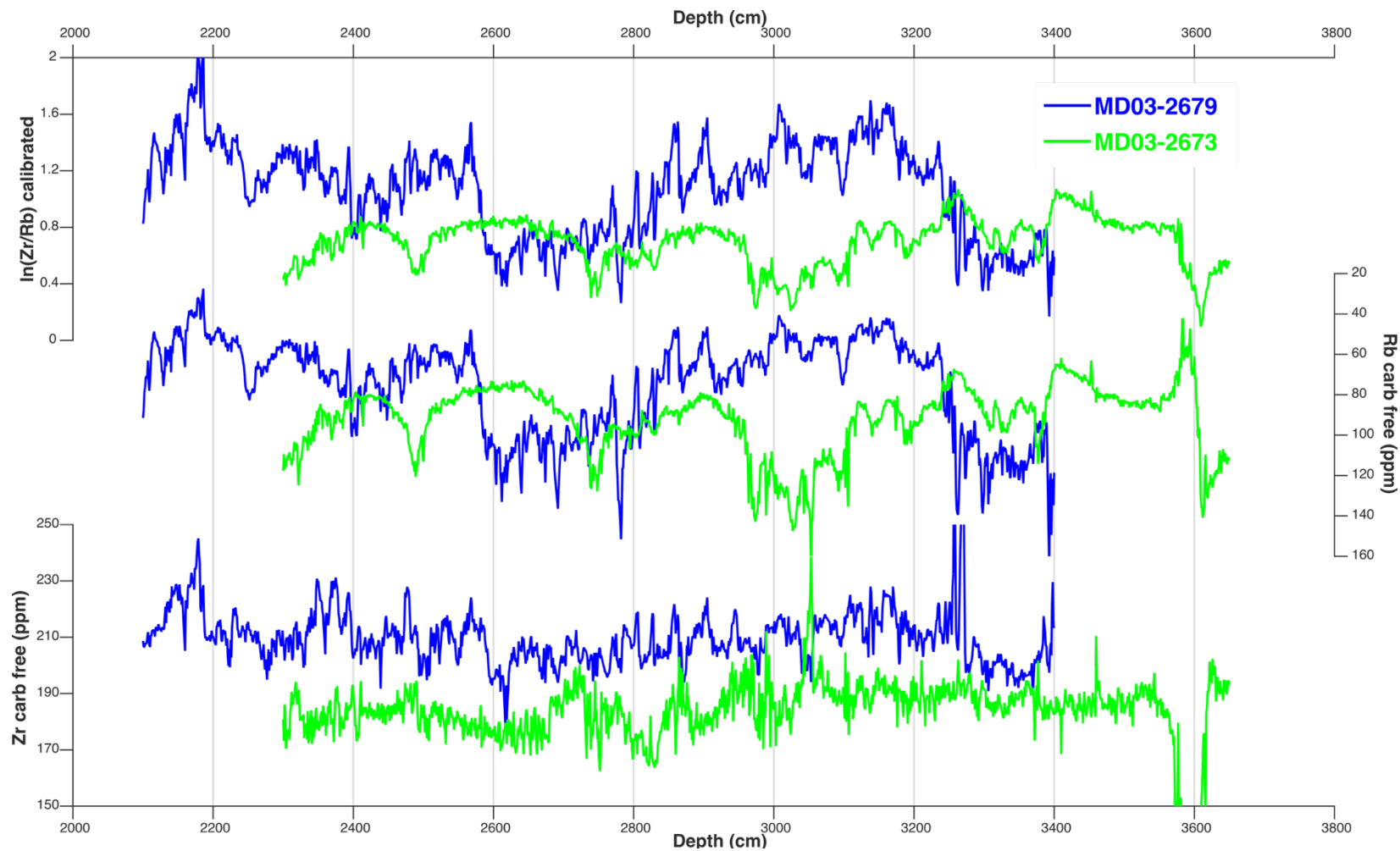


Figure S2. Same as Figure S1 for core MD03-2673.



**Figure S3:** Calibrated concentrations (in %) obtained after running the Multivariate log-ratio calibration (Weltje et al. 2015) in cores (top) MD03-2679 and (bottom) MD03-2673 are plotted versus depth for the ten calibrated elements and the undefined fraction (“Undef”). Note that concentrations on the y-scale are plotted in log-scale.



**Figure S4:** (top)  $\ln(\text{Zr}/\text{Rb})$ , (middle) Rb and (bottom) Zr downcore profiles of calibrated data for cores MD03-2679 (blue) and MD03-2673 (green) on their respective depth scale. Rb and Zr concentrations are expressed in “carbonate free” in order to remove the dilution effect of biogenic carbonates. These concentrations were corrected following the equation given by Poutiers and Gonthier (1978) and Kissel et al. (2013) ( $\text{concentration} \% / 100 - \text{CaCO}_3\%$ ) assuming that Ca concentrations are representative of all biogenic carbonates ( $\text{CaCO}_3$ ). Note that Rb concentrations are plotted in reverse scale.

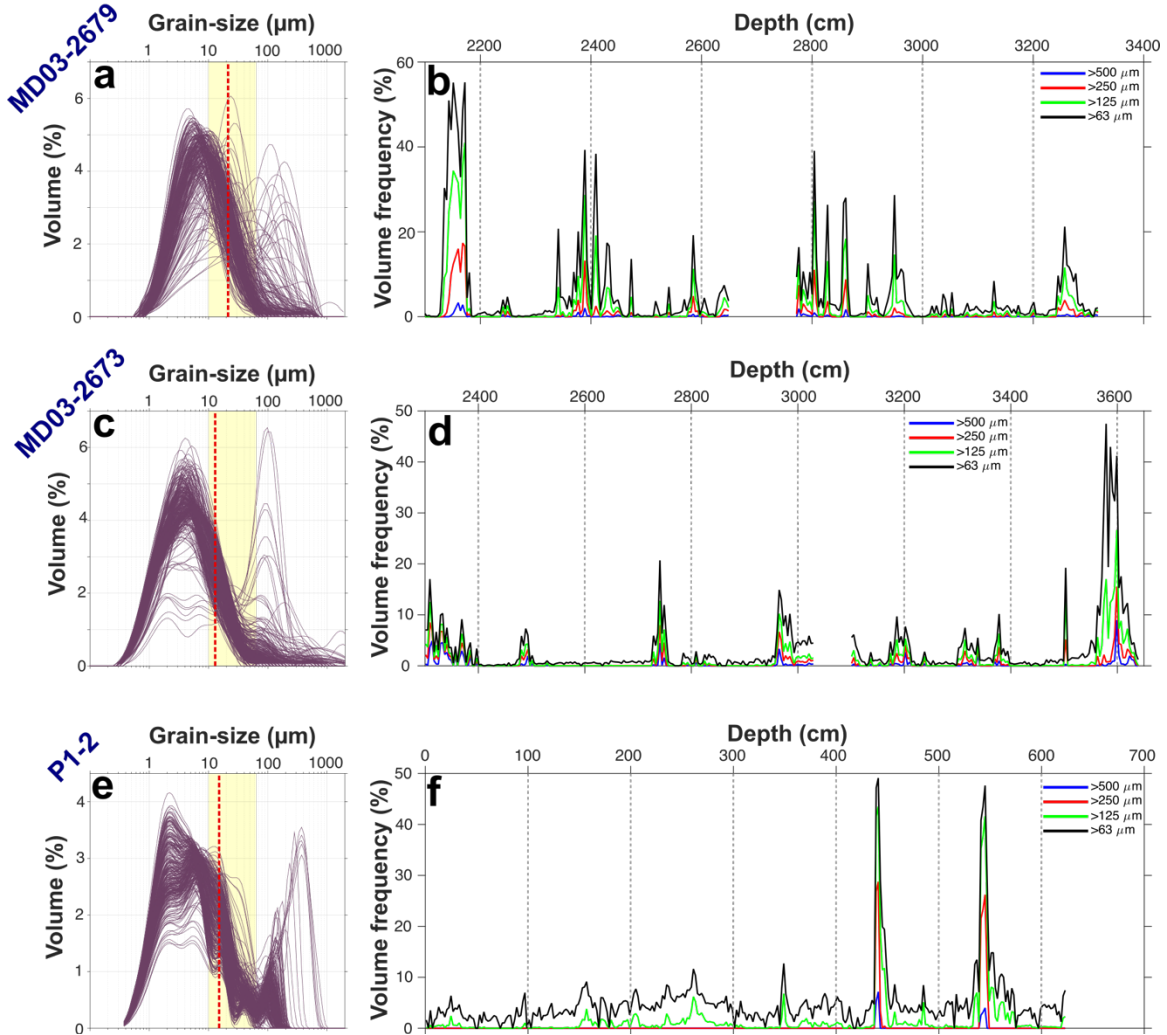


**Figure S5:** Grain-size distributions (a, c, e) and volume frequency (%) sand fraction profiles (b, d, f) of the core MD03-2679 (a, b), core MD03-2673 (c, d) and core ANT30-P1-2 (e, f). The sortable silt interval is marked by light yellow areas in a, c, e. The percentile 80 (i.e. grain-size value below which 80% of the data is, also given in Table 2) of the average grain-size distribution is marked by red dotted lines in a, c, e.